analytical chemistry

pubs.acs.org/ac
Article

Navigating Side Reactions for Robust Colorimetric Detection of Galactose Oxidase Activity

Ying Sin Koo, Adrielle Xianwen Chen, Charlotte Y. J. Tay, Valerie Y. E. Wang, Jie Yang See, Yee Hwee Lim, and Dillon W. P. Tay*

Cite This: Anal. Chem. 2025, 97, 5266−5273
Read Online

ABSTRACT: Colorimetric assays are a rapid, scalable technique well suited to enzyme activity screening. However, side reactions or chromogenic reagent instability can result in false positives or false negatives that compromise the accuracy of such assays. Here, we identify three classes of compounds incompatible with the 2,2′-azino-bis(3-ethylbenzothiazoline-6-sulfonic acid) (ABTS) colorimetric assay for galactose oxidase activity. Dark green $ABTS^{\cdot+}$ cationic radicals indicating enzyme activity can get quenched to yield colorless solutions or couple with substrates to form differently colored adducts, thus preventing accurate colorimetric measurements. These side reactions limit the utility of the ABTS assay and introduce uncertainty in the substrate scope to which it is applicable. We have investigated the underlying mechanisms behind these side reactions to conclude that free radical scavengers, phenols with electron-donating substituents, and β,γ-unsaturated aryl ketones are incompatible with the ABTS colorimetric assay. In search of a viable alternative, we developed an assay using 2,4-dinitrophenylhydrazine under neutral conditions with isopropyl alcohol as a solubilizing agent. The use of neutral conditions was found to be critical to avoid hydrolysis of hydrazone adducts, ensuring reproducible measurements. Our assay is compatible with free radical scavengers (R^2 = 0.98), phenols with electron-donating substituents (R^2 = 0.97), and β,γ-unsaturated aryl ketones (R^2 = 0.88). This modified assay enables galactose oxidase activity screening across a broader substrate scope, thus facilitating enzyme use for more practical applications.

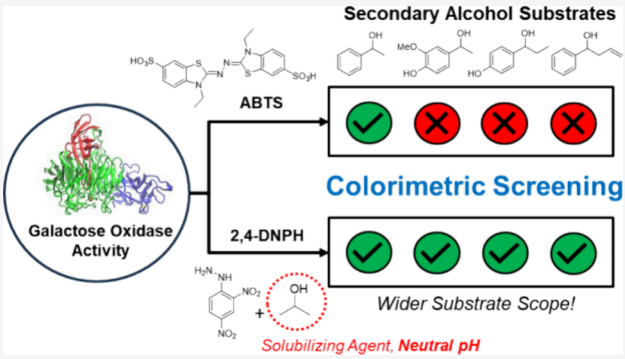

INTRODUCTION

Enzymatic reactions are favored for their exquisite regio- and stereoselectivity, operation under mild reaction conditions, and use of environmentally benign reagents that enable sustainable chemical transformations.[1−3] Their high selectivities minimize byproduct formation, reduce purification costs, increase product yields, and enable multistep biocatalytic cascades in a single pot.[4,5] Overall, enzymatic biocatalysis embodies 10 out of the 12 principles of green chemistry,[6] highlighting its potential to facilitate the transition of chemical manufacturing towards a more sustainable future.[7−10]

Galactose oxidase is an enzyme that catalyzes alcohol oxidation[11,12] to produce aldehydes and ketones that are ubiquitous in high-value specialty chemicals across the agrochemical, flavor, fragrance, and pharmaceutical industries.[13−15] As a demonstration of its utility in sustainable chemical manufacturing, modified galactose oxidase has been employed in the biocatalytic cascade synthesis of an investigational HIV treatment drug, islatravir, with 51% yield[16]—more than double that of state-of-the-art synthetic chemical routes, partially thanks to novel enzymatic selectivity and reactivity halving the number of reaction steps.

Driven by the transformative potential of enzymatic biocatalysis, the development of fast, accurate, and high-throughput screening methods for biocatalytic activity has been garnering interest.[17−20] Enzymes typically require multiple rounds of iterative directed evolution and screening to achieve performance fit for industrial applications.[21−23] In the context of galactose oxidase, biocatalytic activity screening techniques can generally be categorized into two main mechanisms: (1) quantification of the hydrogen peroxide byproduct[24−27] and (2) quantification of the carbonyl product[28,29] (Table S1, Figure 1).

The two essential traits of high-throughput screening assays are (1) speed, to quickly evaluate large enzyme mutant libraries within a reasonable time frame, and (2) accuracy, to correctly identify the best-performing mutants to bring forward to the

Received: December 26, 2024
Revised: January 23, 2025
Accepted: January 30, 2025
Published: February 28, 2025

https://doi.org/10.1021/acs.analchem.4c07034
Anal. Chem. 2025, 97, 5266−5273

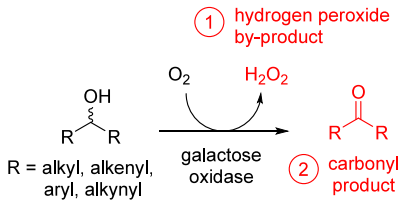

Figure 1. Alcohol oxidation by galactose oxidase and indicators of biocatalytic activity: (1) hydrogen peroxide byproduct and (2) carbonyl product.

next evolution step, accumulating beneficial mutations and improving enzyme activity towards the desired application. In this respect, colorimetric detection stands out as a fast and scalable technique, capable of completing multiple measurements in 96-well plates within seconds. However, side reactions and chromogenic reagent instability can result in unintended byproducts that compromise the accuracy of colorimetric screening. In response to this critical issue, we have embarked on a rigorous exploration of the side reactions during standard[30−32] ABTS colorimetric screening of galactose oxidase activity. Here, we show that free radical scavengers, phenols with electron-donating substituents, and β,γ-unsaturated aryl ketones are incompatible with ABTS, yielding inaccurate results. We then report the development of a viable alternative using 2,4-dinitrophenylhydrazine (2,4-DNPH) under neutral conditions that circumvents these unwanted side reactions and enables reliable colorimetric screening of galactose oxidase activity for these substrates. In particular, the use of neutral conditions was found to be essential for stability and reproducible measurements.

This work provides two key contributions: (1) investigating side reactions to identify substrate classes incompatible with the ABTS assay and (2) developing a viable alternative colorimetric assay that works for these substrate classes. Based on the underlying principles of our developed assay, we anticipate a straightforward generalization to other enzymes operating with similar mechanisms (e.g., cholesterol oxidase,[33] amino acid oxidase,[34] etc.), facilitating the screening of more substrate classes for industrial applications, and contributing to the overarching goal of promoting biocatalysis as a key enabling technology for sustainable chemical manufacturing.

EXPERIMENTAL SECTION

Materials. 4-Phenyl-1-buten-4-ol (S156), 4-(1-hydroxypropyl)-2-methoxyphenol (S157), 1-(*p*-tolyl)but-3-en-1-ol (S167), 4-hydroxypropiophenone (P177), 4-(1-hydroxyethyl)-2-methoxyphenol (S180), 1-(4-hydroxy-3-methoxyphenyl)ethan-1-one (P180), 2,2′-azino-bis(3-ethylbenzothiazoline-6-sulfonic acid) diammonium salt (ABTS), and pyrogallol red were purchased from Merck and used as received. 1-(4-Chlorophenyl)but-3-en-1-ol (S163) was purchased from Combi-Blocks and used as received. Horseradish peroxidase (HRP) was purchased from Toyobo. Purified galactose oxidase mutant GOh1052 was prepared according to the protocol reported in a previous work.[25] Absorption spectra were measured with a Molecular Devices FlexStation 3 Multi-Mode Microplate Reader.

Synthesis of P156, P163, P167, and S177. P156, P163, P167, and S177 were synthesized via known literature procedures.[35−37]

Preparation of the Purple ABTS-S177 Adduct. ABTS (91.3 mg) and HRP (5 mg) were dissolved in ultrapure water (4.534 mL). A H_2O_2 (0.5 M in water, 416 μL) solution was added, and the solution was mixed well to generate dark green $ABTS^{\cdot+}$ radicals. S177 (29 mg) was dissolved in deuterated DMSO (50 μL) and added to the mixture. The dark green solution turned purple upon addition of S177. The mixture was then transferred to a round-bottom flask. Methanol (5 mL) and silica powder (5 g) were added to the flask, and the solvent was removed with a rotary evaporator. The sample was dry loaded for column chromatography and eluted with ethyl acetate/methanol (3:1). Fractions containing the purple adduct (R_f = 0.43) were combined, concentrated, and then redissolved in D_2O (0.5 mL) for NMR analysis. ^{1}H NMR (400 MHz, D_2O): δ 7.98 (1H, d, J = 1.8 Hz), 7.73 (1H, dd, J = 8.6 Hz, 1.8 Hz), 7.44 (1H, d, J = 8.6 Hz), 7.20 (1H, m), 6.94 (1H, dd, J = 9.7 Hz, 2.3 Hz), 6.05 (1H, d, J = 9.7 Hz), 4.35 (2H, m), 4.24 (1H, m), 1.60 (2H, m), 1.39 (3H, t, J = 7.2 Hz), and 0.97 ppm (3H, t, J = 7.3 Hz). HR-MS (+ve ESI): m/z (calcd), $[M + H]^+$ 422.0839; found 422.0845.

ABTS with the P156 Three-Step Color Change. ABTS (0.1 M in ultrapure water, 60 μL) and HRP (1 mg/mL in ultrapure water, 20 μL) were added to ultrapure water (915 μL) to form a pale green solution. P156 (1 M in DMSO, 5 μL) was added, resulting in a dark green solution. The mixture was left to shake (200 rpm) at room temperature for 24 h.

ABTS with P156 under Ambient and Deoxygenated Conditions. ABTS (100 mM in ultrapure water, 650 μL) and HRP (1 mg/mL in 100 mM sodium phosphate pH 7 buffer, 650 μL) were added to sodium phosphate buffer (100 mM, pH 7, 11.7 mL) to yield a (ABTS + HRP) solution. To three round-bottom flasks were added sodium phosphate buffer (100 mM, pH 7, 150 μL) and (ABTS + HRP) solution (1.5 mL) each. One round-bottom flask was then sparged with argon for 2 h, while the other two were capped and left to stand under ambient conditions. Separately, two round-bottom flasks of P156 solution and one DMSO blank were also prepared, each containing sodium phosphate buffer (100 mM, pH 7, 4 mL), as well as P156 (20 mM in DMSO, 500 μL) for P156 solutions or DMSO (500 μL) for the DMSO blank. One flask of P156 solution was sparged with argon for 2 h, while the other was left under ambient conditions. After 2 h, 1.35 mL each of deoxygenated P156 solution and ambient P156 solution were added to the flasks containing the deoxygenated (ABTS + HRP) solution and ambient (ABTS + HRP) solution, respectively. Absorption spectra of the P156 solutions and the DMSO reference blank were taken.

Neutral 2,4-DNPH Colorimetric Assay Calibration Curves. Mixtures mimicking actual galactose oxidase reactions were prepared by combining 2,4-DNPH (5 mM in ethanol, 40 μL), sodium phosphate buffer (100 mM, pH 7, 165 μL), purified galactose oxidase (400 μg/mL in 100 mM sodium phosphate buffer, pH 7, 20 μL), HRP (1 mg/mL in 100 mM sodium phosphate buffer, pH 7, 5 μL), and either DMSO (10 μL) or varying ratios of S180/P180, S177/P177, or S156/P156 (1 mM total concentration in DMSO, 10 μL). The mixture was vortexed briefly and then left to stand for 3 h. Isopropyl alcohol (400 μL for S177/P177 or S156/P156 and 1 mL for S180/P180) was then added, and the solutions were mixed well to dissolve any precipitate. Aliquots (200 μL) were transferred to a clear 96-well plate, and 400 nm absorbance was measured. Calibration curves were constructed with reference to the DMSO blank.

https://doi.org/10.1021/acs.analchem.4c07034
Anal. Chem. 2025, 97, 5266−5273

Calculation of Limit of Detection (LOD) and Limit of Quantification (LOQ). The limit of detection (LOD) was calculated according to IUPAC recommendations[38] (99.86% confidence level). The limit of quantification (LOQ) was calculated according to Regulation (EU) 333/2007.[39]

$$\text{LOD} = 3 \times \frac{\text{standard deviation of blanks}}{\text{slope of calibration curve}} \quad (1)$$

$$\text{LOQ} = 3.3 \times \text{LOD} \quad (2)$$

Neutral 2,4-DNPH Colorimetric Assay for Galactose Oxidase Activity against S177. An S177 sample solution was prepared in an HPLC vial by mixing sodium phosphate buffer (100 mM, pH 7, 135 μL), HRP (1 mg/mL in 100 mM sodium phosphate pH 7 buffer, 5 μL), S177 (20 mM in DMSO, 10 μL), and purified galactose oxidase (400 μg/mL in 100 mM sodium phosphate buffer pH 7, 50 μL). A reference blank solution was prepared by mixing sodium phosphate buffer (100 mM, pH 7, 135 μL), purified galactose oxidase (400 μg/mL in 100 mM sodium phosphate buffer pH 7, 50 μL), HRP (5 μL), and DMSO (10 μL) in an HPLC vial. After shaking at 300 rpm and 25 °C for 24 h, 2,4-DNPH (5 mM in ethanol, 40 μL) was added to each solution before it was left to stand for 3 h. Subsequently, isopropyl alcohol (400 μL) was added to each solution. Aliquots (200 μL) of each solution were transferred to a clear 96-well plate, and their 400 nm absorbance was measured.

RESULTS AND DISCUSSION

ABTS Side Reactions. ABTS colorimetric detection of galactose oxidase activity relies on the interaction between HRP, ABTS, and hydrogen peroxide byproduct from galactose oxidase activity. HRP utilizes hydrogen peroxide to oxidize colorless neutral ABTS molecules (that appear pale green in the bulk solution due to impurities or partial oxidation) to metastable dark green $ABTS^{\cdot+}$ radical cations[27] (Figure 2A). The intensity of this dark green color can be monitored at 420 nm (λ_{max}) to quantify the amount of hydrogen peroxide produced and thus indirectly measure the galactose oxidase activity. Although ABTS has been successfully applied to screen for galactose oxidase activity,[24,25] we have found that it is incompatible with three classes of compounds (Figure 2B).

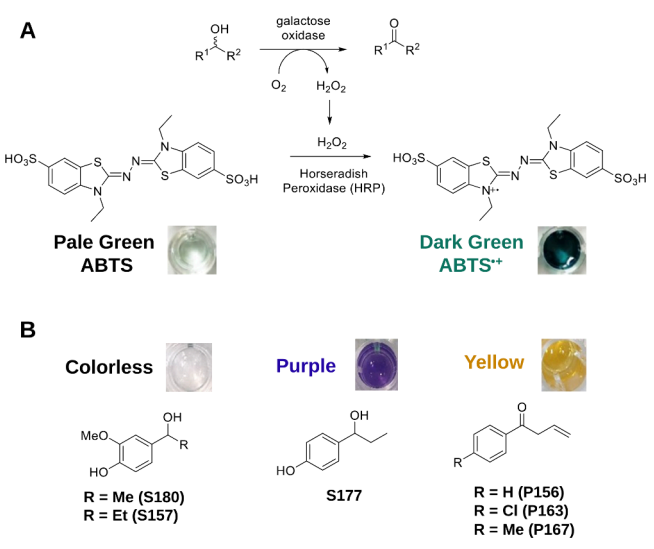

Figure 2. (A) ABTS colorimetric detection of galactose oxidase activity. (B) Three classes of compounds with undesired side reactions with ABTS resulting in decolorization or alternate colors.

Free Radical Scavengers. First, compounds with free radical scavenging properties such as S157 and S180. Free radical scavengers reduce dark green $ABTS^{\cdot+}$ radical cations back to their colorless neutral ABTS form[40] yielding false negatives (Figure S1). This bleaching interaction is known and has been leveraged to measure the antioxidant capacity of compounds via the ABTS/potassium persulfate decolorization assay.[41] However, in the context of colorimetric screening of galactose oxidase activity, such an interaction results in undesired interference and false negatives. By extension, it is expected that compounds with free radical scavenging properties such as analogues of plant polyphenols[42] or highly conjugated alcohols[40] will result in similar undesired decolorization and would thus be incompatible with the ABTS assay.

Phenols with Electron-Donating Substituents. Second, compounds bearing substituted phenols such as S177 (Figure 2B). We propose that phenoxyl radicals are generated from substituted phenols either through direct oxidation[43] by HRP/H_2O_2 or via radical propagation from in situ-formed $ABTS^{\cdot+}$ radicals (Figure 3A). Hydrogen bonding with the aqueous solvent also stabilizes the resulting phenoxyl radical,[44] facilitating its formation. These phenoxyl radicals subsequently couple with $ABTS^{\cdot+}$ radicals in a termination step to yield purple S177-ABTS hydrazindiylidene-like adducts. In-depth characterization via high-resolution electrospray mass spectroscopy (HR-ESI-MS) (Figure S2) and nuclear magnetic resonance (NMR) spectroscopy (Figures S3−S5) corroborates the formation of this purple adduct, which redshifts the absorption spectrum λ_{max} from the expected 420 to 556 nm (Figure 3B). As a result, $ABTS^{\cdot+}$ was depleted, leading to a reduced absorbance at the monitored 420 nm wavelength and a false negative result. This adduct-forming side reaction may be attributed to the weaker O−H bond dissociation energy in phenols substituted with alkyl or alkoxyl groups (78 ∼ 88 kcal mol^{-1})[45] compared to regular O−H bonds (∼105 kcal mol^{-1}, MeOH),[46] thus facilitating homolytic cleavage and subsequent coupling with $ABTS^{\cdot+}$ radicals. Generalizing this principle, substrates bearing phenols with electron-donating substituents are expected to be susceptible to adduct formation and, thus, would be incompatible with the ABTS assay.

***β,γ*-Unsaturated Aryl Ketones.** Third and finally, *β,γ*-unsaturated aryl ketones such as P156, P163, and P167 result in yellow solutions (Figures S6 and S7). Addition of *β,γ*-unsaturated aryl ketones to a solution of ABTS and HRP resulted in a three-step color change (Figure 3C) from (1) dark green to (2) yellow and finally (3) orange, resulting in false negatives. This three-step color change suggests complex reaction kinetics, which have been systematically investigated here with control experiments to deduce the underlying mechanism.

First, a control of ABTS with P156 shows no color change (Figure S7), implying a critical role for HRP in these color changes. Second, when HRP, ABTS, and P156 are combined under anaerobic conditions, no green $ABTS^{\cdot+}$ is formed, unlike the green coloration observed under aerobic conditions (Figure 3D), indicating that atmospheric oxygen is essential for the reaction. Third, addition of P156 quenches dark green $ABTS^{\cdot+}$ solutions to give colorless solutions (Figure S8), suggesting that P156 acts as a single electron donor to reduce $ABTS^{\cdot+}$ radicals. Altogether, these observations point toward

https://doi.org/10.1021/acs.analchem.4c07034
Anal. Chem. 2025, 97, 5266−5273

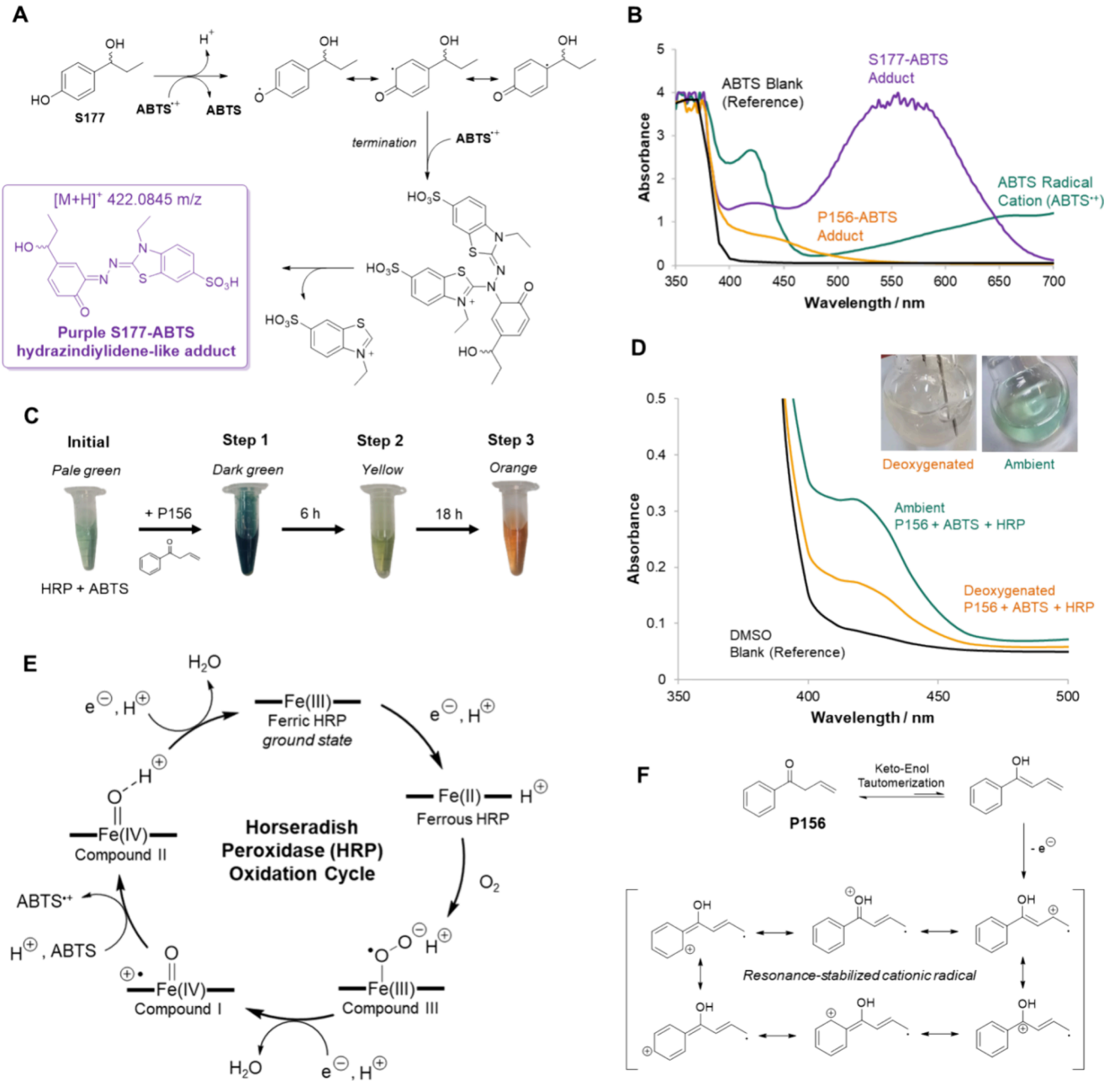

Figure 3. (A) Proposed mechanism for the formation of the purple hydrazindiylidene-like S177-ABTS adduct. (B) Absorption spectra of dark green $ABTS^{\cdot+}$ radical cation, purple S177-ABTS adduct, and orange P156-ABTS adduct versus ABTS blank as a reference. (C) Three-step color change over 24 h upon addition of P156 to a solution of HRP and ABTS. (D) Absorption spectra of deoxygenated and ambient mixtures of P156, HRP, and ABTS immediately after mixing versus DMSO blank as a reference. (E) Catalytic cycle for HRP-mediated aerobic oxidation of ABTS using atmospheric oxygen. (F) Keto−enol tautomerization of P156 and resonance structures of the P156 cationic radical formed after single electron donation.

HRP-mediated aerobic oxidation[47] of ABTS (Figure 3E) with P156 serving as a single electron donor and atmospheric oxygen as the oxidant for the first color change to dark green.

Electron-rich olefins like P156 can act as single electron donors[48] due to their unique traits of (1) keto−enol tautomerization creating an extended conjugated π-electron system and (2) stabilization of the generated cationic radical over their π-electron system (Figure 3F). This allows P156 to perform proton-coupled electron transfer to ground-state ferric HRP, converting it to its ferrous form. Ferrous HRP can then bind atmospheric oxygen to form Compound III with superoxide-like character.[47] Subsequent proton-coupled electron transfer reactions convert Compound III to Compound I, which then oxidizes ABTS to dark green $ABTS^{\cdot+}$ observed in Step 1 with concurrent production of Compound II. Finally, Compound II reverts to ground-state ferric HRP via proton-coupled electron transfer with concomitant release of water, ready to restart the catalytic cycle.

Based on the ability of P156 to quench dark green $ABTS^{\cdot+}$, the second color change should have been from dark green to colorless. However, a yellow color was instead observed. This observation may be attributed to two competing reactions, (1) decolorization via free radical scavenging by P156 and (2) adduct formation via termination between the free radicals

https://doi.org/10.1021/acs.analchem.4c07034
Anal. Chem. 2025, 97, 5266−5273

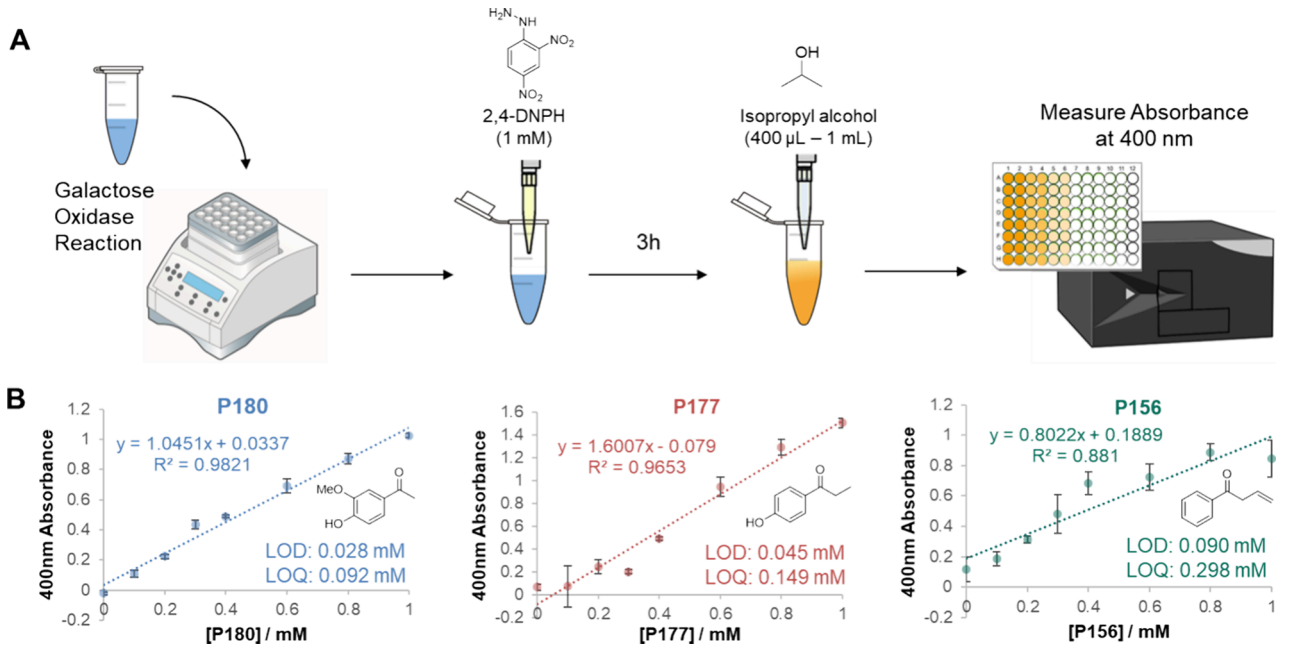

Figure 4. (A) Modified pH-neutral 2,4-DNPH colorimetric galactose oxidase activity assay with isopropyl alcohol as a solubilizing agent. (B) Calibration curves mirroring enzyme reaction conditions for P180, P177, and P156 after subtracting the reference DMSO blank. Error bars of 1 standard deviation shown.

generated in situ from P156 and ABTS. Initially, P156 acts as a single electron donor for HRP-mediated aerobic oxidation of neutral ABTS to yield both $ABTS^{\cdot+}$ and P156 radicals. Dark green $ABTS^{\cdot+}$ radicals produced can then be quenched by P156 back to their colorless neutral forms, regenerating neutral ABTS for further HRP-mediated oxidation while simultaneously creating more P156 radicals. This cycle likely continues until P156 radicals accumulate to a concentration such that reaction kinetics starts to instead favor termination between P156 radicals and ABTS radicals to produce orange P156-ABTS adducts, hypothesized to proceed via a coupling mechanism similar to that of the S177-ABTS adduct. The interplay between (1) HRP-mediated aerobic oxidation of ABTS, (2) quenching of dark green $ABTS^{\cdot+}$ by P156, and (3) P156-ABTS adduct formation in low concentrations would thus explain the observed transition from dark green to yellow instead of dark green to colorless as originally anticipated.

Finally, as the amount of the P156-ABTS adduct accumulates, the color intensifies to yield an orange-colored solution. As supporting evidence, the combination of only P156 with pale green ABTS also turned pale yellow over 24 h, suggesting a reaction between trace amounts of $ABTS^{\cdot+}$ radical present and P156 resulting in a similarly colored adduct. This could be interpreted as radical propagation from $ABTS^{\cdot+}$ to form P156 radicals, followed by termination between $ABTS^{\cdot+}$ and in situ-generated P156 radicals to yield yellow solutions corresponding to a low concentration of the P156-ABTS adduct formed.

Altogether, these would explain the observed three-step color change as (1) HRP-mediated aerobic oxidation of ABTS to dark green $ABTS^{\cdot+}$, (2) quenching of dark green $ABTS^{\cdot+}$ with P156 with simultaneous formation of the P156-ABTS adduct for a yellow solution, and finally (3) accumulation of the P156-ABTS adduct for an orange-colored solution. Overall, β,γ-unsaturated aryl ketones and compounds with extended conjugated systems that are able to act as single electron donors are anticipated to result in similar complications and thus be incompatible with ABTS colorimetric screening.

Modified Neutral 2,4-DNPH Colorimetric Assay. In search of a suitable alternative for these incompatible substrates, pyrogallol red, a direct alternative to ABTS that also measures H_2O_2, was investigated. However, pyrogallol red was found unsuitable due to its instability causing false positives (Figures S9–S11). As the interfering side reactions with ABTS can be traced back to reactions with its cationic radical form, chromogenic agents with an in principle different mechanism from ABTS were also investigated. Among detection methods targeting the carbonyl product, most faced solubility challenges, which we attempted to address. However, issues such as unreactivity and solvatochromism hindered us from obtaining accurate colorimetric results (Figures S12–S15). Ultimately, 2,4-DNPH emerged as a viable alternative, enabling reliable detection through hydrazone formation. Condensation of the carbonyl product to form hydrazones avoids the complicating radical formation step in the ABTS mechanism, circumventing issues with $ABTS^{\cdot+}$ radical quenching, $ABTS^{\cdot+}$ radical coupling, and alternative ABTS oxidation. However, a common limitation of hydrazones for colorimetric screening is their poor aqueous solubility under pH-neutral conditions. Nielsen and co-workers worked around this limitation by adding sulfuric acid as hydrazones have improved solubility under acidic conditions.[28] However, a triplicated calibration curve of acidic 2,4-DNPH with acetone standards shows higher error bars and lower correlations (R^2 = 0.85–0.90) than expected.[28] These measurement variations may be attributed to the susceptibility of the produced hydrazone adducts to acidic hydrolysis,[49] resulting in their degradation and reduced reproducibility. Here, we maintained a neutral pH by employing isopropyl alcohol as a neutral solubilizing agent, solving the solubility issue of hydrazones and enabling robust and reproducible colorimetric quantification of carbonyl products from galactose oxidase reactions

https://doi.org/10.1021/acs.analchem.4c07034
Anal. Chem. 2025, 97, 5266–5273

(Figure 4A). Triplicated neutral 2,4-DNPH assays reliably quantified ketones from all 3 problematic classes in the presence of galactose oxidase, HRP, and corresponding alcohol substrate (Figure 4B, Tables S2 and S3). Calibration curves were constructed mimicking actual reaction conditions, meaning that at all points along the curve, the combined concentration of the alcohol substrate and ketone product remains constant at 1 mM. Consequently, at 0 mM product concentration, the substrate concentration is 1 mM. This may also explain the observed 400 nm absorbance in the P156 calibration curve at 0 mM product. LODs varied from 0.028 to 0.090 mM, while LOQs varied from 0.092 to 0.298 mM across the 3 classes of compounds.

Application Case Study on S177. To demonstrate the utility of the neutral 2,4-DNPH colorimetric assay on a challenging substrate for ABTS, we applied it to activity screening of mutant galactose oxidase oxidation of S177 (Figure 5, Tables S4 and S5). For comparison, we also tested

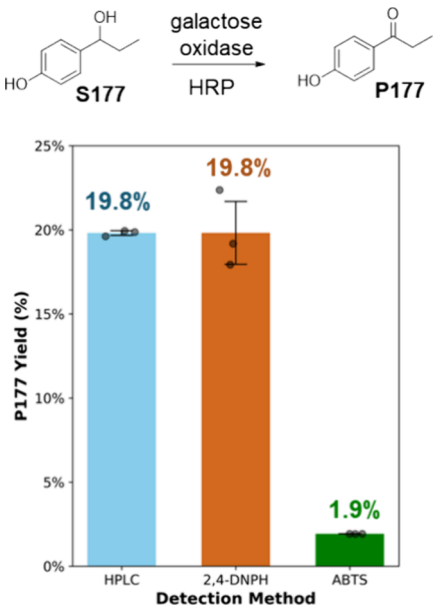

Figure 5. Triplicated mutant galactose oxidase oxidation of S177 quantified via three detection methods of HPLC, 2,4-DNPH, and ABTS. Error bars of 1 standard deviation shown.

the standard ABTS colorimetric assay (Figure S16) under the same conditions. The results were validated using HPLC as a secondary method to quantify the P177 yield (Figure S17).

As anticipated, the ABTS assay produced a false negative, significantly underestimating the P177 yield due to the purple adduct-forming side reactions. In contrast, the modified 2,4-DNPH assay provided results consistent with those of HPLC measurements. Moreover, unlike ABTS that relies on detection of the hydrogen peroxide byproduct, 2,4-DNPH directly quantifies carbonyl products, enabling its generalization to carbonyl-producing enzymes that do not produce hydrogen peroxide as a byproduct (e.g., alcohol dehydrogenase[50]) and even those that use hydrogen peroxide as a reactant (e.g., unspecific peroxygenases[51]).

CONCLUSIONS

The use of ABTS for colorimetric detection of galactose oxidase activity was found to be incompatible with the three compound classes of (1) free radical scavengers, (2) phenols with electron-donating substituents, and (3) β,γ-unsaturated aryl ketones. The interaction of these compounds with either $ABTS^{\cdot+}$ radical cations or neutral ABTS molecules resulted in undesired side reactions and inaccurate measurements. Free radical scavengers quenched dark green $ABTS^{\cdot+}$ radical cations to give colorless solutions. Phenols with electron-donating substituents formed phenoxyl radicals that coupled with $ABTS^{\cdot+}$ radical cations to yield differently colored adducts, and β,γ-unsaturated aryl ketones facilitated HRP-mediated aerobic oxidation, resulting in differently colored solutions. Aside from the three classes investigated here, it should be noted that there may be more interferents (e.g., thiols, amines, etc.) that interact with ABTS, hydrogen peroxide byproduct, or the carbonyl products from galactose oxidase-mediated biocatalytic oxidation, potentially posing challenges to colorimetric detection of galactose oxidase activity. This remains an area for future investigation.

Alternative colorimetric detection methods were investigated, and 2,4-DNPH leveraging isopropyl alcohol as a solubilizing agent was found to be a suitable alternative. The neutral 2,4-DNPH assay demonstrated good reproducibility and correlations (R^2 = 0.881−0.982) for colorimetric quantification of carbonyl products from the three problematic compound classes. This was demonstrated in a case study of mutant galactose oxidase oxidation of S177, where 2,4-DNPH showed P177 yields consistent with HPLC analysis, while ABTS severely underestimated the P177 yield.

Overall, our modified neutral 2,4-DNPH assay enables screening of a broader range of substrates for galactose oxidase and potentially for other enzymes with similar mechanisms, facilitating the development and industrial application of such enzymes. These expanded enzymatic applications are anticipated to enable the replacement of more synthetic chemical processes and to reduce the environmental footprint of chemical manufacturing for a more sustainable future.

ASSOCIATED CONTENT

Supporting Information

The Supporting Information is available free of charge at https://pubs.acs.org/doi/10.1021/acs.analchem.4c07034.

Experimental data from ABTS investigations, investigations on alternative colorimetric detection methods, HRMS data, NMR data, and application case study colorimetric data (PDF)

AUTHOR INFORMATION

Corresponding Author

Dillon W. P. Tay − *Institute of Sustainability for Chemicals, Energy and Environment (ISCE²), Agency for Science, Technology and Research (A*STAR), Singapore 138665, Republic of Singapore*; orcid.org/0000-0002-4831-5525; Email: dillon_tay@isce2.a-star.edu.sg

Authors

Ying Sin Koo − *Institute of Sustainability for Chemicals, Energy and Environment (ISCE²), Agency for Science, Technology and Research (A*STAR), Singapore 138665, Republic of Singapore*

Adrielle Xianwen Chen − *Institute of Sustainability for Chemicals, Energy and Environment (ISCE²), Agency for Science, Technology and Research (A*STAR), Singapore 138665, Republic of Singapore*

https://doi.org/10.1021/acs.analchem.4c07034
Anal. Chem. 2025, 97, 5266−5273

Charlotte Y. J. Tay − *Institute of Sustainability for Chemicals, Energy and Environment (ISCE²), Agency for Science, Technology and Research (A*STAR), Singapore 138665, Republic of Singapore*

Valerie Y. E. Wang − *Institute of Sustainability for Chemicals, Energy and Environment (ISCE²), Agency for Science, Technology and Research (A*STAR), Singapore 138665, Republic of Singapore*

Jie Yang See − *Institute of Sustainability for Chemicals, Energy and Environment (ISCE²), Agency for Science, Technology and Research (A*STAR), Singapore 138665, Republic of Singapore;* orcid.org/0000-0003-1014-190X

Yee Hwee Lim − *Institute of Sustainability for Chemicals, Energy and Environment (ISCE²), Agency for Science, Technology and Research (A*STAR), Singapore 138665, Republic of Singapore; Synthetic Biology Translational Research Program, Yong Loo Lin School of Medicine, National University of Singapore, Singapore 117597, Republic of Singapore;* orcid.org/0000-0002-7789-3893

Complete contact information is available at: https://pubs.acs.org/10.1021/acs.analchem.4c07034

Author Contributions

D.W.P.T. conceptualized, designed, and supervised the study. Y.H.L. conceptualized, supervised, and obtained funding for this work. D.W.P.T., Y.S.K., A.X.C., C.Y.J.T., V.Y.E.W., and J.Y.S. performed the experiments and did data analysis for this study. Y.S.K. and A.X.C. performed the literature review. The manuscript was written through contributions of all authors. All authors have given approval to the final version of the manuscript.

Notes

The authors declare no competing financial interest.

■ ACKNOWLEDGMENTS

We would like to thank Mr. Jeffrey Ng Kang Wai (A*STAR ISCE²) for performing high-resolution mass spectrometry experiments, Ms. Yeo Wan Lin (A*STAR SIFBI) for preparation of the galactose oxidase mutant, Dr. Cheong Choon Boon (A*STAR ISCE²) for assisting with NMR analysis, and funding support from Advanced Manufacturing and Engineering (AME) Industry Alignment Fund Prepositioning (IAF-PP) PIPS (Grant No. A19B3a0009), and Manufacturing Trade and Connectivity (MTC) Individual Research Grant (IRG) (M22K2c0086). J.Y.S. gratefully acknowledges traineeship support from SGUnited.

■ REFERENCES

(1) Alcántara, A. R.; Domínguez de María, P.; Littlechild, J. A.; Schürmann, M.; Sheldon, R. A.; Wohlgemuth, R. *ChemSusChem* **2022**, *15* (9), No. e202102709.

(2) Wu, S.; Snajdrova, R.; Moore, J. C.; Baldenius, K.; Bornscheuer, U. T. *Angew. Chem., Int. Ed.* **2021**, *60* (1), 88−119.

(3) Yi, D.; Bayer, T.; Badenhorst, C. P. S.; Wu, S.; Doerr, M.; Höhne, M.; Bornscheuer, U. T. *Chem. Soc. Rev.* **2021**, *50* (14), 8003−8049.

(4) Sheldon, R. A.; Brady, D. *Chem. Commun.* **2018**, *54* (48), 6088−6104.

(5) Liu, Y.; Liu, P.; Gao, S.; Wang, Z.; Luan, P.; González-Sabín, J.; Jiang, Y. *Chem. Eng. J.* **2021**, *420*, No. 127659.

(6) Ivanković, A.; Dronjić, A.; Bevanda, A. M.; Talić, S. *Int. J. Sustainable Green Energy* **2017**, *6* (3), 39−48.

(7) Sheldon, R. A.; Woodley, J. M. *Chem. Rev.* **2018**, *118* (2), 801−838.

(8) Ran, N.; Zhao, L.; Chen, Z.; Tao, J. *Green Chem.* **2008**, *10* (4), 361−372.

(9) Ferreira-Leitão, V. S.; Cammarota, M. C.; Gonçalves Aguieiras, E. C.; Vasconcelos de Sá, L. R.; Fernandez-Lafuente, R.; Freire, D. M. G. *Catalysts* **2017**, *7* (1), 9.

(10) Bell, E. L.; Finnigan, W.; France, S. P.; Green, A. P.; Hayes, M. A.; Hepworth, L. J.; Lovelock, S. L.; Niikura, H.; Osuna, S.; Romero, E.; Ryan, K. S.; Turner, N. J.; Flitsch, S. L. *Nat. Rev. Methods Primers* **2021**, *1* (1), 46.

(11) Fong, J. K.; Brumer, H. *Essays Biochem.* **2023**, *67* (3), 597−613.

(12) Koschorreck, K.; Alpdagtas, S.; Urlacher, V. B. *Eng. Microbiol.* **2022**, *2* (3), No. 100037.

(13) Birmingham, W. R.; Toftgaard Pedersen, A.; Dias Gomes, M.; Bøje Madsen, M.; Breuer, M.; Woodley, J. M.; Turner, N. J. *Nat. Commun.* **2021**, *12* (1), 4946.

(14) Toftgaard Pedersen, A.; Birmingham, W. R.; Rehn, G.; Charnock, S. J.; Turner, N. J.; Woodley, J. M. *Org. Process Res. Dev.* **2015**, *19* (11), 1580−1589.

(15) Heath, R. S.; Ruscoe, R. E.; Turner, N. J. *Nat. Prod. Rep.* **2022**, *39* (2), 335−388.

(16) Huffman, M. A.; Fryszkowska, A.; Alvizo, O.; Borra-Garske, M.; Campos, K. R.; Canada, K. A.; Devine, P. N.; Duan, D.; Forstater, J. H.; Grosser, S. T.; Halsey, H. M.; Hughes, G. J.; Jo, J.; Joyce, L. A.; Kolev, J. N.; Liang, J.; Maloney, K. M.; Mann, B. F.; Marshall, N. M.; McLaughlin, M.; Moore, J. C.; Murphy, G. S.; Nawrat, C. C.; Nazor, J.; Novick, S.; Patel, N. R.; Rodriguez-Granillo, A.; Robaire, S. A.; Sherer, E. C.; Truppo, M. D.; Whittaker, A. M.; Verma, D.; Xiao, L.; Xu, Y.; Yang, H. *Science* **2019**, *366* (6470), 1255−1259.

(17) Jacques, P.; Béchet, M.; Bigan, M.; Caly, D.; Chataigné, G.; Coutte, F.; Flahaut, C.; Heuson, E.; Leclère, V.; Lecouturier, D.; Phalip, V.; Ravallec, R.; Dhulster, P.; Froidevaux, R. *Bioprocess Biosyst. Eng.* **2017**, *40* (2), 161−180.

(18) Goddard, J.-P.; Reymond, J.-L. *Curr. Opin. Biotechnol.* **2004**, *15* (4), 314−322.

(19) Ye, L.; Yang, C.; Yu, H. *Appl. Microbiol. Biotechnol.* **2018**, *102* (2), 559−567.

(20) Markel, U.; Essani, K. D.; Besirlioglu, V.; Schiffels, J.; Streit, W. R.; Schwaneberg, U. *Chem. Soc. Rev.* **2020**, *49* (1), 233−262.

(21) Turner, N. J. *Trends Biotechnol.* **2003**, *21* (11), 474−478.

(22) Porter, J. L.; Rusli, R. A.; Ollis, D. L. *ChemBioChem.* **2016**, *17* (3), 197−203.

(23) Turner, N. J. *Nat. Chem. Biol.* **2009**, *5* (8), 567−573.

(24) Escalettes, F.; Turner, N. J. *ChemBioChem.* **2008**, *9* (6), 857−860.

(25) Yeo, W. L.; Tay, D. W. P.; Miyajima, J. M. T.; Supekar, S.; Teh, T. M.; Xu, J.; Tan, Y. L.; See, J. Y.; Fan, H.; Maurer-Stroh, S.; Lim, Y. H.; Ang, E. L. *ACS Catal.* **2023**, *13* (24), 16088−16096.

(26) Go, G. Z.; Eggler, A. *Free Radical Biol. Med.* **2017**, *112*, 62.

(27) Abderrahim, M.; Arribas, S. M.; Condezo-Hoyos, L. *Talanta* **2017**, *166*, 349−356.

(28) Kozaeva, E.; Mol, V.; Nikel, P. I.; Nielsen, A. T. *Microb. Biotechnol.* **2022**, *15* (9), 2426−2438.

(29) Li, Z.; Fang, M.; LaGasse, M. K.; Askim, J. R.; Suslick, K. S. *Angew. Chem., Int. Ed.* **2017**, *56* (33), 9860−9863.

(30) Baron, A. J.; Stevens, C.; Wilmot, C.; Seneviratne, K. D.; Blakeley, V.; Dooley, D. M.; Phillips, S. E.; Knowles, P. F.; McPherson, M. J. *J. Biol. Chem.* **1994**, *269* (40), 25095−25105.

(31) Sun, L.; Petrounia, I. P.; Yagasaki, M.; Bandara, G.; Arnold, F. H. *Protein Eng., Des. Sel.* **2001**, *14* (9), 699−704.

(32) Spadiut, O.; Olsson, L.; Brumer, H. *Microb. Cell Fact.* **2010**, *9* (1), 68.

(33) Akanksha; Mishra, V.; Kesari, K. K. Microbial Cholesterol Oxidase: Industrial Applications. In *Microbial Enzymes: Roles and Applications in Industries*, Arora, N. K.; Mishra, J.; Mishra, V., Eds.; Springer Singapore: Singapore, 2020; pp. 303−317.

(34) Curti, B.; Ronchi, S.; Simonetta, M. P. D-and L-amino acid oxidases. In *Chemistry and biochemistry of flavoenzymes*; CRC Press, 2019; pp. 69−94.
(35) Meyer, S. D.; Schreiber, S. L. *J. Org. Chem.* **1994**, *59* (24), 7549−7552.
(36) Kleinmans, R.; Apolinar, O.; Derosa, J.; Karunananda, M. K.; Li, Z.-Q.; Tran, V. T.; Wisniewski, S. R.; Engle, K. M. *Org. Lett.* **2021**, *23* (14), 5311−5316.
(37) Drijfhout, F. P.; Fraaije, M. W.; Jongejan, H.; van Berkel, W. J. H.; Franssen, M. C. R. *Biotechnol. Bioeng.* **1998**, *59* (2), 171−177.
(38) Long, G. L.; Winefordner, J. D. *Anal. Chem.* **1983**, *55* (7), 712A−724A.
(39) Thomas, W.; Haedrich, J.; Alexander, S.; Piotr, R.; Joerg, S. *Guidance Document on the Estimation of LOD and LOQ for Measurements in the Field of Contaminants in Feed and Food*; EUR 28099 EN; Publications Office of the European Union: Luxembourg, 2016.
(40) Nimse, S. B.; Pal, D. *RSC Adv.* **2015**, *5* (35), 27986−28006.
(41) Ilyasov, I. R.; Beloborodov, V. L.; Selivanova, I. A.; Terekhov, R. P. *Int. J. Mol. Sci.* **2020**, *21* (3), 1131.
(42) Kancheva, V. D. *Eur. J. Lipid Sci. Technol.* **2009**, *111* (11), 1072−1089.
(43) Stoyanovsky, D. A.; Goldman, R.; Claycamp, H. G.; Kagan, V. E. *Arch. Biochem. Biophys.* **1995**, *317* (2), 315−323.
(44) Estácio, S. G.; Couto, P. C. d.; Guedes, R. C.; Cabral, B. J. C.; Simões, J. A. M. *Theor. Chem. Acc.* **2004**, *112* (4), 282−289.
(45) Lucarini, M.; Pedrielli, P.; Pedulli, G. F.; Cabiddu, S.; Fattuoni, C. *J. Org. Chem.* **1996**, *61* (26), 9259−9263.
(46) Blanksby, S. J.; Ellison, G. B. *Acc. Chem. Res.* **2003**, *36* (4), 255−263.
(47) Berglund, G. I.; Carlsson, G. H.; Smith, A. T.; Szöke, H.; Henriksen, A.; Hajdu, J. *Nature* **2002**, *417* (6887), 463−468.
(48) Broggi, J.; Terme, T.; Vanelle, P. *Angew. Chem., Int. Ed.* **2014**, *53* (2), 384−413.
(49) Enders, D.; Wortmann, L.; Peters, R. *Acc. Chem. Res.* **2000**, *33* (3), 157−169.
(50) Milagre, C. D. F.; Milagre, H. M. S. *Curr. Opin. Green Sustainable Chem.* **2022**, *38*, No. 100694.
(51) Kinner, A.; Rosenthal, K.; Lütz, S. *Front. Bioeng. Biotechnol.* **2021**, *9*, No. 705630.

https://doi.org/10.1021/acs.analchem.4c07034
Anal. Chem. 2025, 97, 5266−5273